

## The Role of Sodium Carbonate and Oxides Supported on Lanthanide Oxides in the Oxidative Dimerization of Methane

YUdong TONG, MICHAEL P. ROSYNEK, AND JACK H. LUNSFORD

*Department of Chemistry, Texas A & M University, College Station, Texas 77843*

Received May 21, 1990

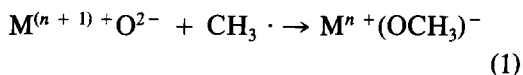
The addition of Na<sub>2</sub>CO<sub>3</sub> to three representative lanthanide oxides, La<sub>2</sub>O<sub>3</sub>, CeO<sub>2</sub>, and Yb<sub>2</sub>O<sub>3</sub>, has a marked effect on the catalytic properties of these materials for the oxidative dimerization of methane. The effect is most dramatic for CeO<sub>2</sub>, which, upon addition of Na<sub>2</sub>CO<sub>3</sub>, is transformed from a total oxidation catalyst to one which is reasonably selective for the conversion of CH<sub>4</sub> to C<sub>2</sub>H<sub>4</sub> and C<sub>2</sub>H<sub>6</sub>. Results obtained by X-ray photoelectron spectroscopy and ion scattering spectroscopy show that a sodium carbonate/sodium oxide phase largely covers the lanthanide oxide surface, thus the catalytic properties are those of the sodium phase, rather than those of the lanthanide oxide. Indeed, the specific activities of the Na<sup>+</sup>/Ln<sub>x</sub>O<sub>y</sub> catalysts and of pure Na<sub>2</sub>CO<sub>3</sub> were the same within a factor of 2.5, with Na<sup>+</sup>/Yb<sub>2</sub>O<sub>3</sub> at the high end of the range. The specific activities of pure lanthanide oxides were considerably greater than those of the modified catalysts. Although Na<sub>2</sub>CO<sub>3</sub> is the principal compound present on the surface of the Na<sup>+</sup>/Ln<sub>x</sub>O<sub>y</sub> catalysts, it is probable that Na<sub>2</sub>O<sub>2</sub> is responsible for the activation of CH<sub>4</sub>. © 1990 Academic Press, Inc.

### INTRODUCTION

The lanthanide oxides differ greatly with respect to their ability to catalyze the oxidative dimerization of methane (1, 2); however, when these oxides are modified with alkali metal ions, their differences are often less apparent. The properties of these oxides in the partial oxidation of methane have been reviewed recently by Hutchings *et al.* (3). Since the goal of most of the previous research has been to optimize the selectivity or the yield of ethane and ethylene (C<sub>2</sub> products), the reaction have often been carried out under conditions of high oxygen conversion, making it difficult to extract intrinsic activities from the data.

We have shown that the large differences in C<sub>2</sub> selectives observed among various members of the lanthanide oxide series result mainly from secondary reaction between CH<sub>3</sub>· radicals and the metal oxide (4). Those oxides which have accessible multiple cationic oxidation states (CeO<sub>2</sub>,

Pr<sub>6</sub>O<sub>11</sub>, and Tb<sub>4</sub>O<sub>7</sub>) react with CH<sub>3</sub>· radicals, presumably by the reaction



and the resulting surface methoxide ions provide a route to the formation of CO<sub>2</sub>. In the absence of such secondary reactions, the CH<sub>3</sub>· radicals couple to form the desired C<sub>2</sub> products.

When CeO<sub>2</sub> is modified by the addition of Na<sub>2</sub>CO<sub>3</sub>, it ceases to be a good radical scavenger, and becomes an effective catalyst for the production of gas phase CH<sub>3</sub>· radicals (4). These changes are paralleled by its transformation from a total CH<sub>4</sub> oxidation catalyst to one that is effective in the oxidative coupling reaction. Similar changes in selectivity have been reported by Gaffney *et al.* (5) for the catalytic properties of Pr<sub>6</sub>O<sub>11</sub> before and after its modification with sodium salts.

Quite different behaviors are exhibited by the other members of the lanthanide oxide

series, of which  $\text{La}_2\text{O}_3$  and  $\text{Yb}_2\text{O}_3$  are examples of the extremes. Lanthanum oxide is very effective in the formation of gas phase  $\text{CH}_3 \cdot$  radicals, and, consistent with this fact, it is a poor radical scavenger (4). Ytterbium oxide is neither a good radical producer nor a good radical scavenger.

In our previous study, it was noted that a sodium carbonate/sodium oxide phase largely covered the  $\text{CeO}_2$  surface and that the specific activity of nominally pure  $\text{Na}_2\text{CO}_3$  for the generation of  $\text{CH}_3 \cdot$  radicals approached that of the  $\text{Na}^+/\text{CeO}_2$  catalyst (4). These preliminary observations suggested that the lanthanide oxide may serve primarily as a support for an active form of sodium oxide. In order to determine the validity of this hypothesis, three diverse members of the lanthanide oxide series ( $\text{La}_2\text{O}_3$ ,  $\text{CeO}_2$ , and  $\text{Yb}_2\text{O}_3$ ), both with and without added sodium, were evaluated with respect to their catalytic performances and their abilities to generate gas-phase  $\text{CH}_3 \cdot$  radicals. With the sodium-modified catalysts, care was taken to operate under conditions of moderate  $\text{CH}_4$  and  $\text{O}_2$  conversions, so that the specific activities of the catalysts could be compared.

#### EXPERIMENTAL

**Catalyst preparation.** The starting materials were  $\text{Na}_2\text{CO}_3$  (99.999%),  $\text{La}_2\text{O}_3$  (99.99%),  $\text{CeO}_2$  (99.9%), and  $\text{Yb}_2\text{O}_3$  (99.9%), and were obtained from Aldrich Chemical Co. The sodium-doped lanthanide oxide catalysts,  $\text{Na}^+/\text{Ln}_x\text{O}_y$ , were made by dissolving sodium carbonate in deionized water, adding the appropriate amount of  $\text{Ln}_x\text{O}_y$  to the solution, and then evaporating the water with vigorous stirring until a thick paste was formed. The paste was dried at  $120^\circ\text{C}$  overnight and then calcined at  $700^\circ\text{C}$  in air for 10 h. This calcination step is necessary to achieve stable activities of the catalysts. Before contacting with reactant, the catalysts were pretreated in flowing  $\text{O}_2$  at temperatures close to or greater than the operational temperatures, e.g.,  $780^\circ\text{C}$  for  $\text{Na}^+/\text{CeO}_2$ . The sodium content is ex-

pressed as the weight percentage of sodium in the lanthanide oxide, and was determined using inductively coupled plasma (ICP) emission spectroscopy. Pure  $\text{La}_2\text{O}_3$ ,  $\text{CeO}_2$ , and  $\text{Yb}_2\text{O}_3$  were treated in the same manner, but without the addition of sodium.

**Catalytic experiments.** The catalytic data were obtained using conventional flow reactors constructed of alumina (Omegatite 450, 99.8%  $\text{Al}_2\text{O}_3$ ). One reactor was 3.2-mm i.d. in the region where the catalyst was located, and immediately below the catalyst bed a four-holed alumina insert (3.2-mm o.d., 0.5-mm-diameter holes) was used to reduce the time that the product stream remained in the heated region of the system. A 0.050 g catalyst bed was supported between thin layers of quartz wool. Above the catalyst was a layer of quartz chips that served to preheat the gases and to minimize the purely homogeneous reactions. Blank runs, in which the catalyst was replaced by quartz chips, showed negligible conversion in the oxidation of methane. A bare thermocouple coated with a thin layer of an inert cement was placed inside the catalyst bed via two of the holes in the exit tube.

A second reactor was 10-mm i.d., and a two-holed alumina insert (6.4-mm o.d., 1.5-mm-diameter holes) was placed below the catalyst bed, as shown in Fig. 1. Except for larger dimensions and a larger catalyst bed (0.50 g), this reactor was essentially the same as the one described above. A coated thermocouple located in the center of the catalyst bed was used to measure the temperature ( $T_{\text{in}}$ ) during reaction, and a bare thermocouple on the outside of the reactor was used to control the temperature ( $T_{\text{out}}$ ).

The system was allowed to reach steady state, which was usually ca. 10 h after initial exposure to the reactants, before the data reported here were obtained. Product gas analyses were performed using a conventional gas chromatographic (GC) technique. A thermal conductivity detector was used to analyze for  $\text{CH}_4$ ,  $\text{O}_2$ ,  $\text{C}_2\text{H}_4$ ,  $\text{C}_2\text{H}_6$ ,  $\text{CO}$ , and  $\text{CO}_2$ , while propane and butane

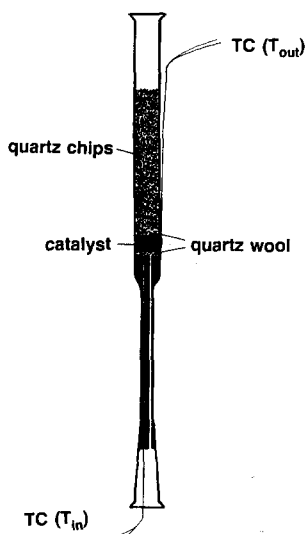


FIG. 1. Alumina reactor used to obtain the data at high levels of oxygen conversion.

were analyzed using a flame ionization detector. The gases used to make up the feed gas were  $\text{CH}_4$  (Matheson, 99.97%),  $\text{O}_2$  (Matheson, 99.6%), and He (Airco, 99.99%).

**ESR experiments.** The matrix isolation electron spin resonance (MIESR) system used in this study has been described in detail previously (6). A flow reactor containing a layer of the catalyst of interest was coupled to the MIESR system. The gases exiting from the catalyst were allowed to leak into a low pressure collection region where part of the methyl radicals were frozen onto a cold (14 K) sapphire rod. The rod was then lowered into the ESR cavity, and the spectrum was recorded. This system was used to determine the activities of the  $\text{Na}^+/\text{Ln}_x\text{O}_y$  catalysts, as well as those of the pure compounds, for the formation of gas phase  $\text{CH}_3 \cdot$  radicals. The catalysts studied in the MIESR system were steady-state catalysts from the conventional reactors. A typical procedure for the MIESR experiment involved retreating the sample at elevated temperatures in  $\text{O}_2$  for 1 h, evacuating the gas phase for 10 min, and then admitting the reactants. The time interval between the

introduction of reactants and the beginning of a collection of  $\text{CH}_3 \cdot$  radicals was 1 h. The relative concentration of the gas phase  $\text{CH}_3 \cdot$  radicals was determined from the signal intensity of the ESR spectrum of the  $\text{CH}_3 \cdot$  radicals.

**Characterization techniques.** Powder X-ray diffraction (XRD) patterns were obtained with a computer-controlled Seifert-Scintag Pad II automated powder diffractometer, using  $\text{CuK}\alpha$  radiation. The crystalline phases present in the catalysts were determined after various treatments.

The near-surface compositions of the  $\text{Na}^+/\text{Ln}_2\text{O}_3$  catalysts were determined by X-ray photoelectron spectroscopy (XPS) on a Hewlett-Packard Model HP5950A instrument, using monochromatic  $\text{AlK}\alpha$  excitation. Used catalyst samples were further heated *in vacuo* at 250–300°C for about 10 h to remove adsorbed water and weakly bound carbon dioxide. The samples were then pressed into wafers and loaded into the spectrometer without exposure to the atmosphere. The regions scanned covered the 1s binding energies of oxygen, carbon, and sodium, as well as the 3d binding energies of La and Ce and the 4d binding energy of Yb. Adventitious carbon with an assigned binding energy of 285 eV was used as an internal standard to determine the binding energies of the other species. Ion scattering spectroscopy (ISS), which is highly surface sensitive technique, was used to determine the composition of the top layer of a used  $\text{Na}^+/\text{CeO}_2$  catalyst. ISS data were obtained on a Leybold MAX-200 spectrometer at a fixed retardation ratio of 4, using 2.3 keV  $^4\text{He}^+$  ions.

The surface areas of the catalysts were determined using a dynamic BET system from Quantachrome Corp., with nitrogen as the adsorbate. For those materials of low surface area ( $< 0.5 \text{ m}^2/\text{g}$ ), such as  $\text{Na}_2\text{CO}_3$ , a 2 to 3-g sample was used in the measurement to reduce the error caused by the low surface area. In addition, the surface area of the sample tube used in the measurements was determined and subtracted from the val-

ues obtained for those materials. Although the systematic error may be somewhat larger, the relative errors (repeatability) for surface areas measured in the same system were approximately  $\pm 0.02 \text{ m}^2/\text{g}$  for samples having an area  $< 0.5 \text{ m}^2/\text{g}$  and  $\pm 0.04 \text{ m}^2/\text{g}$  for samples having an area  $> 0.5 \text{ m}^2/\text{g}$ .

## RESULTS AND DISCUSSION

**Characterization.** Both the fresh and used  $\text{Na}^+/\text{Ln}_x\text{O}_y$  catalysts exhibited the same XRD patterns, and the only crystalline phases detected in the catalysts were the corresponding lanthanide oxides; no new crystalline species, such as  $\text{Na}_2\text{CeO}_3$  or  $\text{NaYbO}_2$ , were found. It is a little surprising that crystalline phases due to sodium carbonate or the oxides of sodium were not observed by XRD, when one considers the amount of  $\text{Na}_2\text{CO}_3$  added to the catalysts. Failure to observe a phase that corresponds to a sodium compound suggest that the sodium carbonate existed as very small crystallites or as a thin layer on the surfaces of the lanthanide oxides. These results may be contrasted with those obtained on a used  $\text{Na}^+/\text{CaO}$  catalyst, for which a distinct  $\text{Na}_2\text{CO}_3$  phase was observed (7).

As an example of the XPS results, the spectra of 4%  $\text{Na}^+/\text{CeO}_2$  which had been used in a catalytic test are shown in Fig. 2. In this O 1s region, three peaks may be resolved, at binding energies of 529, 532, and 534 eV. Comparison of these results with the XPS spectra of  $\text{CeO}_2$ ,  $\text{Na}_2\text{CO}_3$ ,  $\text{NaHCO}_3$ , and  $\text{Na}_2\text{O}_2$  indicate that the peaks at 529 and 532 eV may be assigned to  $\text{O}^{2-}$  and to oxygen in  $\text{CO}_3^{2-}$ , respectively. The broad peak at 532 eV may include contributions from  $\text{OH}^-$  and even  $\text{O}_2^{2-}$  oxygen. The broader shoulder at 534 eV is tentatively assigned to oxygen present in  $\text{HCO}_3^-$  ions. The presence of  $\text{CO}_3^{2-}$  is supported by a C 1s peak at 289 eV. The  $\text{HCO}_3^-$  species, if present, should have resulted in a C 1s line at 289 eV, but this peak may have been below the limits of detection (8).

From the areas under the Na 1s and the Ln 3d and 4d peaks, with appropriate cor-

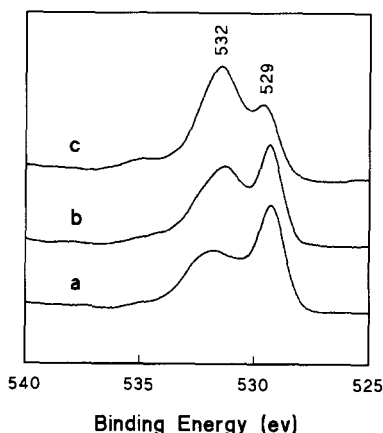


FIG. 2. XPS spectra in the O(1s) region of 4%  $\text{Na}^+/\text{CeO}_2$  catalyst after (a) calcination in air at  $700^\circ\text{C}$  for 16 h, (b) further calcination in  $\text{O}_2$  at  $780^\circ\text{C}$  for 2 h, and (c) use as a catalyst at  $780^\circ\text{C}$  for 17 h.

rections for cross sections, the atomic ratios of the metal ions in the near-surface region were determined for the used catalysts, and these are compared with the bulk atomic ratios from ICP analyses in Table 1. Clearly, the Na : Ln ratios are greater at the surface than in the bulk for all three catalysts, with the ratio being greatest for the 4%  $\text{Na}^+/\text{CeO}_2$  catalyst. The ISS results shown in Fig. 3 confirm that a phase containing sodium ions completely covered the used 4%  $\text{Na}^+/\text{CeO}_2$  catalyst. Initially, almost no Ce ions were detected on the surface; only  $\text{Na}^+$  ions were observed. After several minutes of ion etching, however, the underlying Ce ions began to appear. These ISS results are con-

TABLE 1

Na : Ln Atomic Ratios Determined by XPS and ICP<sup>a</sup>

Catalyst	Na : Ln at surface (XPS)	Na : Ln in bulk (ICP)
4% $\text{Na}^+/\text{La}_2\text{O}_3$	1.0	0.29
4% $\text{Na}^+/\text{Yb}_2\text{O}_3$	0.9	0.26
4% $\text{Na}^+/\text{CeO}_2$	3.7	0.24

<sup>a</sup> Used catalysts:  $\text{Na}/\text{La}_2\text{O}_3$ ,  $730^\circ\text{C}$  for 10 h;  $\text{Na}/\text{Yb}_2\text{O}_3$ ,  $760^\circ\text{C}$  for 11 h;  $\text{Na}/\text{CeO}_2$ ,  $780^\circ\text{C}$  for 17 h.

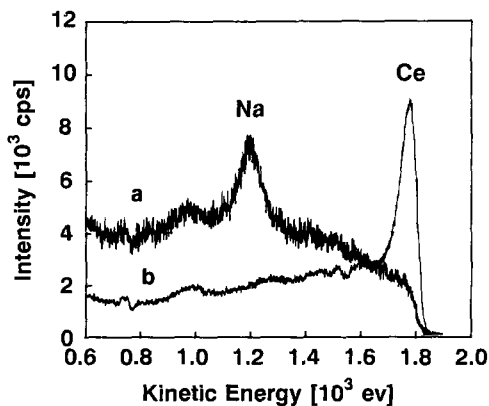


FIG. 3. ISS spectra of (a) pure  $\text{CeO}_2$  and (b) a used 4%  $\text{Na}^+/\text{CeO}_2$  catalyst.

sistent with the previous catalytic experiments which demonstrated that the addition of  $\text{Na}_2\text{CO}_3$  transformed  $\text{CeO}_2$  from a totally nonselective  $\text{CH}_4$  oxidation catalyst to one which gave ca. 60% selectivity to higher hydrocarbons (4). Moreover, it was observed that  $\text{CeO}_2$  was transformed from a good  $\text{CH}_3 \cdot$  radical scavenger to a good generator of gas phase  $\text{CH}_3 \cdot$  radicals.

A calculation of a hypothetical uniform layer of  $\text{Na}_2\text{CO}_3$  on a 4%  $\text{Na}^+/\text{CeO}_2$  catalyst shows that the thickness would be about 400 Å, which corresponds to about 90 layers of the carbonate. Obviously, if such a uniform layer existed, then no Ce would have been evident in the XPS spectrum. We conclude, therefore, that the used  $\text{Na}^+/\text{CeO}_2$  catalyst was completely, but nonuniformly, covered with sodium compounds that include sodium carbonate and sodium oxides, particularly under reaction conditions.

It was found that the atomic ratios, determined from the XPS spectra, strongly depended on the nature of the support and on the previous history of the catalyst. The changes in surface stoichiometry of 4%  $\text{Na}^+/\text{CeO}_2$  catalyst and a 4%  $\text{Na}^+/\text{Yb}_2\text{O}_3$  catalyst were determined as a function of the catalyst treatment. After calcination in air at 700°C for 16 h, both catalysts exhibited a Na : Ln ratio of about 1.2. After being used

in the catalytic reaction for 17–20 h at 780°C, the Na : Ln ratio increased to 3.7 for  $\text{Na}^+/\text{CeO}_2$ , but decreased to 0.5 for  $\text{Na}^+/\text{Yb}_2\text{O}_3$ . It is not clear whether the decrease observed with the latter catalyst resulted from loss of  $\text{Na}_2\text{CO}_3$  from the surface or whether agglomeration, rather than spreading of the  $\text{Na}_2\text{CO}_3/\text{Na}_2\text{O}_2$ , occurred. In either case, it is evident that  $\text{CeO}_2$  has a stronger affinity than  $\text{Yb}_2\text{O}_3$  for surface sodium compounds.

The effect of sample treatment on the spreading of  $\text{Na}_2\text{CO}_3$ , and perhaps of  $\text{Na}_2\text{O}_2$ , over  $\text{CeO}_2$  is also evident in the O 1s spectra of Fig. 2. Exposure of the catalyst to  $\text{O}_2$  and then to reactants at 780°C caused an increase in intensity of the peak at 531–532 eV, relative to the peak at 529 eV. Moreover, there was a distinct shift of the broad maximum at about 532 eV to a sharper maximum at 531 eV. This shift is consistent with the partial transformation of  $\text{Na}_2\text{CO}_3$  (532 eV) to  $\text{Na}_2\text{O}_2$  (531 eV) (9). These results support the postulate that  $\text{CeO}_2$ , which has an  $\text{O}^{2-}$  peak at 529 eV, is covered by sodium compounds which are characterized by O 1s peaks at 531–532 eV.

**Catalytic results.** Prior to carrying out specific activity measurements the three lanthanide oxide catalysts, with and without added sodium carbonate, were studied under nearly oxygen-limiting conditions, and the results are summarized in Table 2. The sodium-modified catalysts are characterized by  $\text{C}_2^+$  selectivities of 52–57% and by productivities which compare favorably with most of the more active catalysts that have been reported (3). The productivities given here and elsewhere may be misleading, however, since the systems are nearly oxygen limited. Pure  $\text{La}_2\text{O}_3$  was somewhat less selective than 4%  $\text{Na}^+/\text{La}_2\text{O}_3$ , while pure  $\text{CeO}_2$ , as noted previously, produced mainly  $\text{CO}_2$  and  $\text{H}_2\text{O}$ . The conversions and selectivities for  $\text{Na}^+/\text{La}_2\text{O}_3$  are comparable to those reported previously by DeBoy and Hicks (10) at somewhat greater temperatures and space velocities. We are not aware of any comparable study of  $\text{Na}^+/\text{Yb}_2\text{O}_3$ .

In contrast to this work, 4%  $\text{Na}^+/\text{CeO}_2$

TABLE 2  
Performances of  $\text{Na}_2\text{CO}_3$ ,  $\text{Ln}_x\text{O}_y$ , and  $\text{Na}^+/\text{Ln}_x\text{O}_y$  Catalysts

Catalyst <sup>a</sup>	$\text{O}_2$ Conv. %	$\text{CH}_4$ Conv. %	$\text{C}_2^+$ Sel. %	Partial pressure, Torr					$\text{C}_2^+$ Prod. <sup>b</sup>
				$\text{C}_2\text{H}_4$	$\text{C}_2\text{H}_6$	$\text{C}_4\text{H}_{10}$	CO	$\text{CO}_2$	
$\text{Na}_2\text{CO}_3$	10	5.3	47.8	0.9	3.2	0.1	2.8	6.6	0.08
$\text{La}_2\text{O}_3$	>99	25.1	46.2	10.4	9.9	0.8	7.8	43.2	0.38
$\text{CeO}_2$	100	13.7	1.2	0.0	0.3	0.0	0.0	51.0	0.01
$\text{Yb}_2\text{O}_3$	83	20.1	40.3	6.5	7.3	0.5	9.0	34.8	0.27
4% $\text{Na}^+/\text{La}_2\text{O}_3$	73	21.8	56.8	9.6	12.2	1.0	2.2	34.0	0.41
4% $\text{Na}^+/\text{CeO}_2$	81	21.7	52.7	8.2	12.1	0.8	0.0	39.3	0.38
4% $\text{Na}^+/\text{Yb}_2\text{O}_3$	81	21.9	52.3	8.3	12.1	0.8	2.3	38.2	0.38

<sup>a</sup> 0.50 g of 20–40 mesh catalyst chips was loaded into an 11 mm i.d.  $\text{Al}_2\text{O}_3$  reactor. Total flow rate = 84 ml/min;  $\text{CH}_4:\text{O}_2 = 5.5:1$ ;  $P(\text{CH}_4) = 0.5$  atm;  $T_{\text{in}} = 775^\circ\text{C}$ ;  $P_{\text{total}} = 1$  atm.

<sup>b</sup>  $\text{C}_2^+$  productivity:  $\text{g}(\text{CH}_4 \text{ to } \text{C}_2^+)/\text{g}(\text{catalyst})/\text{h}$ .

has been reported to be quite a poor catalyst in the redox mode (5). We tested our  $\text{Na}^+/\text{CeO}_2$  catalyst in the redox mode and found it to be nearly as productive as in the co-feed mode. This discrepancy in results probably arises from variations in the method of preparation, including the calcination temperature.  $\text{CeO}_2$  has been used in automotive emission control catalysts because of its ability to store and release oxygen in a redox process (11, 12), and it has been reported that the oxygen storage capacities of  $\text{CeO}_2$  and of noble metal/ $\text{CeO}_2$  catalysts change with pretreatment temperature. For example, a general decrease in the oxygen storage capacity of the catalysts was observed when the calcination temperature was increased from 600 to 800°C (11). The poor redox mode performance of the 4%  $\text{Na}^+/\text{CeO}_2$  catalyst reported previously (5) may have resulted from its calcination at 900°C for 16 h before testing.

The sodium-promoted catalysts and pure  $\text{Na}_2\text{CO}_3$  were also studied under nearly differential conditions so that their specific activities could be more meaningfully compared, and the results are reported in Table 3. Results for the pure lanthanide oxides are also reported in Table 3, but over these catalysts the reactions were oxygen limited. Obviously, the conditions chosen for the

data of Table 3 were not those that would give maximum  $\text{C}_2^+$  selectivities or yields. Here, it should be noted that  $\text{C}_2\text{H}_4$  and  $\text{C}_2\text{H}_6$  were the major  $\text{C}_2^+$  products, and the amount of higher hydrocarbons was less than 5% of the total. From the results in Table 3, it is apparent that the addition of sodium carbonate to a lanthanide oxide decreased both the percent conversion and the specific activity per unit surface area.

In Table 3, the specific activities are compared for four  $\text{Na}^+/\text{Ln}_x\text{O}_y$  catalysts and for nominally pure  $\text{Na}_2\text{CO}_3$  under the same conditions. Although the total activities of these catalysts (based on  $\text{CH}_4$  conversion) varied by a factor of more than 40, the specific activities varied by a factor of only 2.5. If one considers the catalysts 4%  $\text{Na}^+/\text{CeO}_2$ , 10%  $\text{Na}^+/\text{CeO}_2$ , and  $\text{Na}_2\text{CO}_3$ , the specific activities were virtually identical. These results are consistent with the observation that sodium compounds essentially cover the  $\text{CeO}_2$  surface, and therefore the observed reaction rate might be expected to reflect the activity of this sodium carbonate/sodium oxide phase. The specific activity of the  $\text{Na}^+/\text{La}_2\text{O}_3$  catalyst was slightly greater than those of the latter three catalysts, but was substantially less than that of the pure  $\text{La}_2\text{O}_3$ . We conclude, therefore, that the activity of this catalyst was also largely a result

TABLE 3  
Catalytic Properties of  $\text{Ln}_x\text{O}_y$ ,  $\text{Na}_2\text{CO}_3$ , and  $\text{Na}/\text{Ln}_x\text{O}_y$  for Methane Coupling

Catalyst	$\text{CH}_4$ Conv. <sup>a</sup> (%)	$\text{C}_2^+$ Prod. <sup>b</sup>	Surface Area ( $\text{m}^2/\text{g}$ )	Specific Activity (per unit area)	$[\text{CH}_3 \cdot]^c$
$\text{La}_2\text{O}_3$	21.9 <sup>d</sup>	3.08	2.2	(10.0) <sup>d</sup>	4.4
$\text{CeO}_2$	11.0 <sup>d</sup>	0.0	2.5	(4.6) <sup>d</sup>	0.0
$\text{Yb}_2\text{O}_3$	17.3	1.97	1.8	9.6	1.1
$\text{Na}_2\text{CO}_3$	0.2	0.02	0.08	3.0	3.7
4% $\text{Na}/\text{La}_2\text{O}_3$	6.1	0.75	1.5	4.1	3.3
4% $\text{Na}/\text{CeO}_2$	2.5	0.23	0.84	3.0	3.6
4% $\text{Na}/\text{Yb}_2\text{O}_3$	8.7	0.95	1.3	6.5	4.6
10% $\text{Na}/\text{CeO}_2$	3.5	0.28	1.2	2.9	2.3

<sup>a</sup> 0.050 g catalyst chips in a 3-mm i.d.  $\text{Al}_2\text{O}_3$  reactor; WHSV =  $25.7 \text{ h}^{-1}$ ;  $P(\text{CH}_4) = 0.5 \text{ atm}$ ;  $\text{CH}_4:\text{O}_2 = 5:1$ ; Temperature =  $730^\circ\text{C}$ ; Pressure = 1 atm.

<sup>b</sup>  $\text{C}_2^+$  productivity,  $\text{g}(\text{CH}_4 \text{ to } \text{C}_2^+)/\text{g}(\text{catalyst})/\text{h}$ .

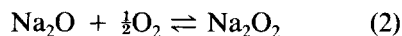
<sup>c</sup> Relative rate of  $\text{CH}_3 \cdot$  radical formation,  $\text{m}^{-2} \cdot \text{s}^{-1}$ : 0.30 g catalyst;  $P = 1.5 \text{ Torr}$ ;  $T = 730^\circ\text{C}$ ; Flow rates, (ml/min): He 3.9;  $\text{CH}_4$  1.2;  $\text{O}_2$  0.028.

<sup>d</sup> Under  $\text{O}_2$ -limited conditions.

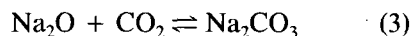
of the sodium carbonate/sodium oxide phase. The specific activity of the  $\text{Na}^+/\text{Yb}_2\text{O}_3$  catalyst was somewhat greater than expected on the basis of the  $\text{Na}_2\text{CO}_3$  activity, which might indicate an incomplete coverage of  $\text{Yb}_2\text{O}_3$  by the sodium compounds.

The abilities of the catalysts to generate gas phase  $\text{CH}_3 \cdot$  radicals also parallel the specific activities of the  $\text{Na}_2\text{CO}_3$  and the  $\text{Na}^+/\text{Ln}_x\text{O}_y$  catalysts; thus, we conclude that a mechanism involving the role of surface-generated gas-phase radicals is common to all of these catalysts. The agreement between the  $\text{CH}_4$  conversion and the  $\text{CH}_3 \cdot$  radical production over the pure lanthanide oxides is not as good, however, and may reflect the oxygen-limiting conditions. As observed previously,  $\text{CeO}_2$  did not produce any gas phase  $\text{CH}_3 \cdot$  radicals, which is consistent with the absence of  $\text{C}_2^+$  products.

Although the  $\text{Na}^+/\text{Ln}_x\text{O}_y$  catalysts were largely covered by a sodium carbonate/sodium oxide phase, we believe that the sodium oxide component, probably  $\text{Na}_2\text{O}_2$ , is responsible for the activation of  $\text{CH}_4$ . A representation of such a catalyst is given in Fig. 4. Here,  $\text{Na}_2\text{O}$  is in equilibrium with  $\text{Na}_2\text{O}_2$  through the reaction



Otsuka and co-workers (13) have provided convincing evidence that  $\text{Na}_2\text{O}_2$  is capable of stoichiometrically converting  $\text{CH}_4$  to  $\text{C}_2$  products at temperatures as low as  $400^\circ\text{C}$ . By contrast, the formation of  $\text{Na}_2\text{CO}_3$  via the equilibrium reaction



has an adverse effect both on the generation of  $\text{CH}_3 \cdot$  radicals and on the conversion of  $\text{CH}_4$  (14, 15). In view of the similarity in specific activities of  $\text{Na}_2\text{CO}_3$ ,  $\text{Na}^+/\text{CeO}_2$ , and  $\text{Na}^+/\text{La}_2\text{O}_3$ , one may conclude that the

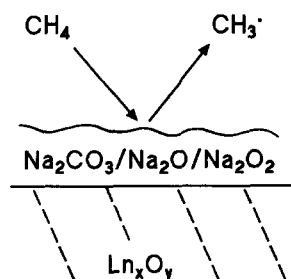


FIG. 4. Scheme of  $\text{Ln}_x\text{O}_y$  catalyst covered with sodium compounds.

lanthanide oxide does not significantly influence this equilibrium.

In many respects, the concepts introduced here extend and confirm the model developed by Gaffney *et al.* (5) to explain the catalytic properties of  $\text{Na}^+/\text{Pr}_6\text{O}_{11}$ . According to that model,  $\text{CH}_4$  is activated by  $\text{Na}_2\text{O}_2$ , and the regeneration of  $\text{Na}_2\text{O}_2$  is facilitated by a rapid  $\text{Pr}^{3+} \rightleftharpoons \text{Pr}^4$  redox couple. In view of this study and our previous paper (4), it also seems that the presence of a sodium carbonate/sodium oxide phase on the surface prevents  $\text{CH}_3 \cdot$  radicals from reacting with  $\text{Pr}_6\text{O}_{11}$ , which would result ultimately in the formation of  $\text{CO}_2$ .

Finally, it should be pointed out that the present model does not preclude the activation of  $\text{CH}_4$  by centers of the type  $[\text{Na}^+\text{O}^-]$  that are formed, for example, when  $\text{Na}^+$  substitutes for  $\text{Ca}^{2+}$  ions in  $\text{CaO}$  (7). Important distinctions between the predominance of  $[\text{Na}^+\text{O}^-]$  or  $\text{Na}_2\text{O}_2$  as centers for the activation of  $\text{CH}_4$  can be made on the basis of (i) a suitable match between the guest and host ionic radii and (ii) the temperature at which good  $\text{C}_2$  selectivity is attained. The formation of centers of the type  $[\text{M}^+\text{O}^-]$  requires that the ionic radius of the alkali metal ion be less than or equal to the size of the metal ion in the host oxide. Furthermore, the presence of  $\text{Na}_2\text{O}_2$  under steady-state reaction conditions requires that the equilibrium of reaction (3) be shifted to the left. Thus,  $\text{Na}_2\text{O}$ , and presumably  $\text{Na}_2\text{O}_2$ , is favored by higher temperatures. The importance of these factors is illustrated by the two catalysts  $\text{Li}^+/\text{MgO}$  and  $\text{Na}^+/\text{MgO}$ . The former is characterized by  $[\text{Li}^+\text{O}^-]$  centers and high  $\text{C}_2$  yields at temperatures  $\leq 720^\circ\text{C}$  (16). Moreover, the conversion of  $\text{Li}_2\text{O}$  to  $\text{Li}_2\text{CO}_3$  has almost no effect on  $\text{C}_2$  productivity (17). By contrast,  $\text{Na}^+/\text{MgO}$  has no  $[\text{Na}^+\text{O}^-]$  centers because of the mismatch in ionic size, and the catalyst changes from

a poor one for oxidative coupling at  $\leq 700^\circ\text{C}$  to a relatively good one at  $750^\circ\text{C}$  (18, 19).

#### ACKNOWLEDGMENTS

We acknowledge financial support of this work by the Division of Chemical Sciences, Office of Basic Energy Sciences, U.S. Department of Energy.

#### REFERENCES

- Otsuka, K., Jinno, K., and Morikawa, A., *J. Catal.* **100**, 353 (1986).
- Campbell, K. D., Zhang, H., and Lunsford, J. H., *J. Phys. Chem.* **92**, 750 (1988).
- Hutchings, G. J., Scurrall, M. S., and Woodhouse, J. R., *Chem. Soc. Rev.* **18**, 251 (1989).
- Tong, Y., Rosynek, M. P., and Lunsford, J. H., *J. Phys. Chem.* **93**, 2896 (1989).
- Gaffney, A. M., Jones, C. A., Leonard, J. J., and Sofranko, J. A., *J. Catal.* **114**, 422 (1988).
- Martir, W., and Lunsford, J. H., *J. Amer. Chem. Soc.* **103**, 3728 (1981).
- Lin, C.-H., Wang, J., and Lunsford, J. H., *J. Catal.* **111**, 302 (1988).
- Kharas, K. C. C., and Lunsford, J. H., *J. Amer. Chem. Soc.* **111**, 2336 (1989).
- The O 1s binding energies of  $\text{Na}_2\text{CO}_3$  and  $\text{Na}_2\text{O}_2$  were determined in our laboratory by K. C. C. Kharas.
- DeBoy, J. M., and Hicks, R. F., *J. Chem. Soc. Chem. Commun.*, 982 (1988).
- Yao, A. C., and Yu Yao, Y. F., *J. Catal.* **86**, 254 (1984).
- Loof, P., Kasemo, B., and Keek, K.-E., *J. Catal.* **118**, 339 (1989).
- Otsuka, K., Said, A. A., Jinno, K., and Komatsu, T., *Chem. Lett.* **77**, (1988).
- Campbell, K. D., and Lunsford, J. H., *J. Phys. Chem.* **92**, 5792 (1988).
- Korf, S. J., Roos, J. A., deBruijn, M. A., van Ommen, J. G., and Ross, J. R. H., *J. Chem. Soc. Chem. Commun.*, 1433 (1987).
- Ito, T., Wang, J.-X., Lin, C.-H., and Lunsford, J. H., *J. Amer. Chem. Soc.* **107**, 5062 (1985).
- Lunsford, J. H., Cisneros, M. D., Hinson, P. G., Tong, Y., and Zhang, H., *Faraday Discuss. Chem. Soc.* **87**, paper 219 (1989).
- Lin, C.-H., Ito, T., Wang, J.-X., and Lunsford, J. H., *J. Amer. Chem. Soc.* **109**, 4808 (1987).
- Iwamats, E., Moryama, T., Takasaki, N., and Aika, K., *J. Chem. Soc. Chem. Commun.* **19** (1986).